International Journal of Smart Home
Vol. 10, No. 9 (2016), pp. 169-178
http://dx.doi.org/10.14257/ijsh.2016.10.9.16

Analysis on Slope Stability of Open Pit Coal Mine Based on Grey Support Vector Machine

Liu Bo[1], Zhang Peng[1, 2] and Zhang Jianwei[2]

[1.] *School of Mechanics and Civil Engineering, China University of Mining & Technology (Beijing), Beijing, 100083, China*
[2.] *Department of Planning and Engineering, Shenhua Baorixile Energy Co.Ltd, Hulunber 021000, China*
438033324@qq.com

Abstract

Shenhua BaoRi XiLe open-pit coal mine slope is located in the seismic belt of hulunbuir prairie in Inner Mongolia, which belongs to the high frequency and intensity earthquake zone, with rainfall concentrated, poor geological distribution, under the influence of complex environmental factors, extremely easy to cause landslide. This paper uses grey model and support vector machine (SVM) to establish slope model, and carries out stress and strain characteristics under the condition of natural, rainfall, earthquake and calculation and analysis of stability. Through the experiment, it analyzes the stability coefficient of downhill under rainfall condition, and obtains the different strength reduction of safety factor list. At the same time, give full consideration to the uncertainty of the earthquake, assume a variety of working conditions of the earthquake, it conducts dynamic analysis of the slope in detail, and gets the dynamic characteristics curves of the monitoring points. Results show that, relative complex terrain conditions, climate conditions and at a high intensity earthquakes area, are the main factors to induce landslides in this region. Therefore, this paper provides a reliable basis for further study of the effects of rainfall and earthquake on slope and disaster prevention and mitigation.

Keywords: *Slope; Coal mine;Rainfall; Landslide ;Stability;The numerical simulation*

1. Introduction

At present, the landslide and debris flow have been gradually affected the safety of people's life and property. Rainfall and earthquake are the main factors that triggered landslide. Therefore, it is particularly important to study the stability of slope under multiple conditions. At present, the study of slope stability under single condition emerged in endlessly. At the present stage, less research on the slope stability under multiple conditions. On the basis of a number of existing studies, with shearer open-pit coal mine slope as an example, combined the characteristics of various numerical analyzing methods, this paper carries out the study of slope stability under multiple conditions as natural, rainfall and earthquake and engineering safety evaluation, which provide the basic data and related technical basis for the safety study of the slope under multiple conditions.

2. Numerical Modeling

2.1. Basic Information of Model

It adopts Finite difference 3D model for slope research, the model is 180 m long, 80 m wide, and 110 m tall. Average gradient is about 0.48. The middle-upper part of the slope is the easy landslide area, gradient is about 36 °. For convenience of analysis, take section

ISSN: 1975-4094 IJSH

1-1along the axis of symmetry of easy landslide area, axis of symmetry of landslide area has 51 ° Angle to the due north direction.

2.2. Interior Structure Plane Division

Model is consisted of four structural planes. Structural plane Ⅰ is the interface of sandstone, killas chip limestone and upper mass rock and soil and gravelly soil, with tilt Angle of 40 °; structural plane Ⅱ is the interface of gravelly soil and mass rock and soil, with tilt Angle of 16 °; structural plane Ⅲ is the interface of mass rock and soil and silty clay, with tilt Angle of 34 °; structural plane IV is the interface of silty clay and upper cladding soil, with tilt Angle of 38 °. Structural plane Ⅰ starting around the bottom extends to structural plane Ⅳ, while structural plane Ⅳ from the top extends to the bottom of the slope, structural plane Ⅱ and Ⅲ locate between Ⅰ and Ⅳ.Four structural planes divide the slope into three parts, the bulk mass part at the bottom is the sandstone, killas chip limestone, on which is small volume of gravel soil and sickle shaped mass rock and soil, on the top is silty clay. According to acquired data of field survey, the physical and mechanical parameters of slope rock and soil are shown in table 1, the slope model diagram as shown in Figure 1:

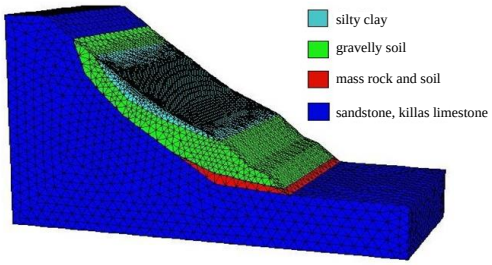

Figure 1. Slope Model Diagram

2.3. Meshing and Boundary Settings

Slope model unit adopts 8-point regular tetrahedron, model is consisted of 20761 unit points, and 99422 unit bodies, easy 5 times encryption on landslide part, can better simulate the change condition of layers. Under the natural and rainfall conditions, add fixed boundaries at the bottom and all around of the model. Under earthquake condition, add free field boundary at all around of model, it can better simulate the infinite far field and the absorption of seismic waves.

2.4. Working Conditions

For Shenhua BaoRi XiLe open-pit coal mine slope is located in the seismic belt of hulunbuir prairie in Inner Mongolia, with soft quality of rock in the area, poor geological distribution, it can cause rock and soil lateral and leads to slight landslides under natural conditions.

Changing climate in this region, rainfall concentrated, rainwater infiltrate into the soil after rainstorm, and long-term rainfall, it greatly increases the quality of soil on the slope, softens the filler in cracks or some of the weak intercalation, thus produces hydrostatic pressure, and reduces the quality of soil and stability of rock on the slope, which lead to the occurrence of disasters such as collapse, landslides and debris flows.

Seismic zone in Inner Mongolia is a high-intensity frequent earthquake area, under the seismic action, because of the poor geologic factors such as collapse, strewn at random,

dangerous falling rocks, big (giant) type of landslide, *etc*., and secondary disaster of numerous mud-rock flow due to heavy rainfall concentrated, therefore, the dynamic characteristics analysis on this slope under natural, rainfall and earthquake conditions is particularly important.

3. Calculation of Various Working Conditions and Result Analysis

3.1. Prediction Model

GM (1, 1) is the most common and simple grey model, composed by a differential equation containing only single variable model, is a special case of GM (1, N). Set the original data sequence as GM (1, 1) modeling sequence $x^{(0)}$, namely

$$x^{(0)} = (x^{(0)}(1), x^{(0)}(2), \ldots, x^{(0)}(n)) \tag{1}$$

$x^{(0)}$ using one-accumulation to generate 1-AGO sequence and set as $x^{(1)}$, then we have

$$x^{(1)} = (x^{(1)}(1), x^{(1)}(2), \ldots, x^{(1)}(n)) \tag{2}$$

Where, $x^{(1)}(1) = x^{(0)}(1)$; $x^{(1)}(k) = \sum_{m=1}^{k} x^{(0)}(m)$。Let $z^{(1)}$ as the mean value sequence of $x^{(1)}$, and the $z^{(1)}$ is obtained as

$$z^{(1)}(k) = 0.5x^{(1)}(k) + 0.5x^{(1)}(k-1) \tag{3}$$

Then, grey differential equation model of GM(1,1) is

$$x^{(0)}(k) + az^{(1)}(k) = b \tag{4}$$

Substitute $k = 2,3,...,n$ into the above formula, then we have

$$\begin{cases} x^{(0)}(2) + az^{(1)}(2) = b \\ x^{(0)}(3) + az^{(1)}(2) = b \\ \vdots \quad \vdots \quad \vdots \quad \vdots \\ x^{(0)}(4) + az^{(1)}(2) = b \end{cases} \tag{5}$$

The above equation can be converted as matrix equation as follows

$$y_N = BP = [x^{(0)}(2), x^{(0)}(3), ..., x^{(0)}(n)]^T \tag{6}$$

Where , B denotes data matrix, y_N denotes data vector, P denotes parameter vector, and

$\begin{cases} B = \begin{bmatrix} -z^{(1)}(2) & 1 \\ -z^{(1)}(3) & 1 \\ \ldots & \ldots \\ -z^{(1)}(n) & 1 \end{bmatrix} \\ P = [a,b] \end{cases}$. Using the least square method for solution to get:

$$P = (a,b)^T = (B^T B)^{-1} B^T y_N \tag{7}$$

To substitute the obtained factor $P = [a,b]$ into formula (4), then solving differential equation, can obtain the content type expression of gray GM(1,1).

$$\hat{x}^{(0)}(k) = u^{k-2} \cdot v \tag{8}$$

Where, $u = \frac{1-0.5a}{1+0.5a}$, $v = \frac{b - a \cdot x^{(0)}(1)}{1+0.5a}$. Then perform tests, let $\varepsilon(k)$ as residual error, that is

$$\varepsilon(k) = \frac{x^{(0)}(k) - \hat{x}^{(0)}(k)}{x^{(0)}(k)} \times 100\% \tag{9}$$

It requires $\varepsilon(k) \le 20\%$ in general, $\varepsilon(k) \le 10\%$ is the best.

The more complex of the corresponding quadratic programming problem solved by support vector machine (SVM), the slower of calculation speed it is, the least squares support vector machine (LSSVM) makes improvement on support vector machine, so the complexity of solving is reduced, therefore this research adopts the LSSVM as prediction model. For network public time series, the LSSVM regression function is

$$f(x) = w^T \varphi(x) + b \tag{10}$$

Where, ω denotes weight vector, b denotes offset.

To introduce structure risk function, and formula (10) is converted to quadratic optimization

$$\min \|w\|^2 + \frac{1}{2}\gamma \sum_{i=1}^{n} \xi_i^2 \tag{11}$$

The constraint condition as

$$y_i = w^T \varphi(x) + b + \xi_i \tag{12}$$

Where, γ represents regularization parameter； ξ_i represents slack variable.

To introduce lagrangian multiplier, and obtain

$$\begin{aligned} L(w,b,\zeta,\alpha) = \frac{1}{2}w^T w + \frac{1}{2}\gamma \sum_{i=1}^{n} \zeta_i^2 + \\ \sum_{i=1}^{n} \alpha_i (w^T \varphi(x_i) - b + \xi_i - y_i) \end{aligned} \tag{13}$$

Where, α_i represents lagrangian multiplier,

Based on KKT condition to obtain

$$\frac{\partial L}{\partial w} = 0, \frac{\partial L}{\partial b} = 0, \frac{\partial L}{\partial \xi_i} = 0, \frac{\partial L}{\partial \alpha_i} = 0 \tag{14}$$

therefore, the final solution can be obtained as:

$$\begin{bmatrix} 0 & 1^T \\ 1 & x^t x + \gamma^{-1} I \end{bmatrix} \begin{bmatrix} a \\ b \end{bmatrix} = \begin{bmatrix} 0 \\ y \end{bmatrix} \tag{15}$$

Introduce kernel function k(xi,xj) to make conversion of formula (15), and the LSSVM prediction model is obtained as:

$$f(x) = \sum_{i=1}^{n} \alpha_i k(x_i, x_j) + b \tag{16}$$

This study adopts RBF function as LSSVM kernel function, finally the LSSVM prediction model is obtained as:

$$f(x) = \sum_{i=1}^{N} \alpha_i \exp\left(-\frac{\|x_i - x_j\|^2}{2\sigma^2} \right) + b \tag{17}$$

Where, σ2 is kernel bandwidth of RBF.

From the LSSVM regression modeling process, the LSSVM model based on radial basis kernel function parameters required to be determined are(γ, σ2), select LSSVM parameters with common n fold cross-validation method, but in the presence of a set of validation parameters, its calculation amount is too large, convergence speed is slow, parameters obtained by cross validation method may not be the optimal solution. Therefore, using cross validation method is difficult to obtain optimal LSSVM model. Genetic algorithm has stronger global searching ability, so genetic algorithm is adopted to define the parameters of LSSVM.

3.2. Rainfall Condition

In the simulation, considering the influence of different rainfall on the slope, it simulates two rainfall conditions of 25mm/d and 50mm/d, and considering the softening effects of parameters such as bulk modulus, shear modulus, friction Angle, cohesive force, with 0.85, 0.72 times reduction. At the same time, considering the load effect of infiltration water under the rainfall condition, it adopts density increasing method, to expand the bulk density. Using the self-made strength reduction, the slope safety factors under various conditions are obtained by calculation as shown in table 1.

It can be known from table 1 and Figure 2 that, when no reduction, the safety factor of slope is 1.318, and the safety reserve is higher, landslides will not generated. When the rainfall is 25mm/d, safety factor Ks is 1.001, reduced by 24.23% compared with that of natural condition. Sliding bodies are concentrated on the central and upper part of the slope, high displacement area is distributed within elevation of 2683-2714m, and the maximum displacement is about 3.93 cm. The shear strain increment peak of slope is 1.600×10-2-1.671×10-2. Compared with natural condition, shear strain increment of slope shall be increased, further extended to the foot of slope, and shear and strain increment shall be cut-through the slope at this moment. It is characterized that safety reserve of the slope is running out in 25 mm/d rainfall condition, the slope is in a critical state of landslide, the small increase of rainfall or slight vibration can activate landslides. When rainfall is up to 50mm/d, safety factor Ks is 0.906, safety reserve is 0, it is reduced by 31.26% compared with previous values, the sliding body are concentrated on a large area in the middle of the slope, high displacement area is distributed in elevation range of 2680-2735m, the maximum total displacement is about 55.62 cm, the shear and strain increment peak of slope is 6.000×10-2-6.819×10-2. Compared with the natural condition, the shear and strain peak is mutated, the high value range increases, a new shear strain increment high displacement area is formed in the middle-lower part of slope, further extended to the foot of slope, and shear and strain increment shall be cut-through the slope. It is characterized the slope is destroyed, and local landslide is generated.

It can be known from analysis, compared with rainfall condition and natural condition, the location of high displacement area is roughly the same, but with the increase of rainfall, the softening effect of water on soil is strengthening, and the stability reduces gradually, and direction scope of high displacement area increasing faster along the slope surface, the normal direction along the slope has slight decrease. In 50mm/d rainfall condition, the slope deformation is increased obviously by 3.93 cm to 55.62 cm, characterization of slope is damaged due to combined action of soil softening of rainwater infiltration and bulk density increasing, which is consistent with the actual engineering situation.

3.3. Seismic Condition

3.3.1. Seismic Condition Analysis

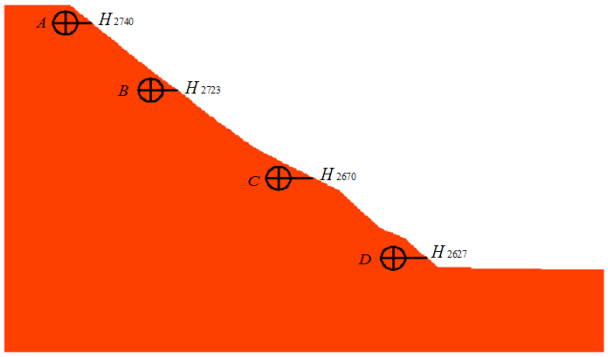

Figure 2. Monitoring Location Map

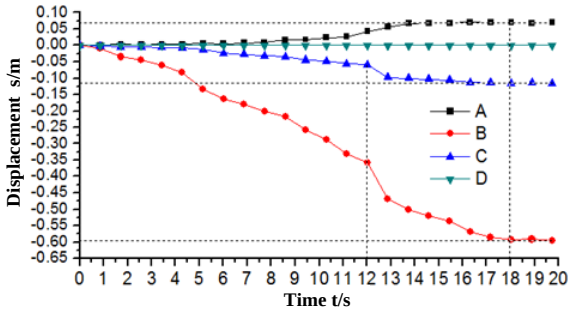

Figure 3. Displacement Diagram of each Monitoring Point of Seismic Condition of Hulunbuir Pasture Land

To arrange 4 monitoring points in the I-I profile of model, the specific locations (as shown in Figure g): monitoring pint A at the 2740m elevation, monitoring pint at the 2723m elevation, monitoring pint C at the 2670m elevation, and monitoring pint D at the 2627 elevation. The acceleration, velocity, displacement and other characteristics of each monitoring point is recorded accordingly.

It can be known from Figure 3 that, the displacement of point D is the minimum, almost to be zero; Point A begins to move at 3.5s, and mutates at 11s, and achieves maximum 7.5 cm at 14 s; point C begins to move at 3.5 s, mutates at 12s, and achieves maximum 12.5cm at 17s; the displacement changes of point B are the largest within 1s-18s, and achieves maximum 59cm at 18s. Each monitoring point reaches the stable state at 18s, characterization the plastic deformation of each monitoring point under the seismic action, destruction happens near slope waist point B.

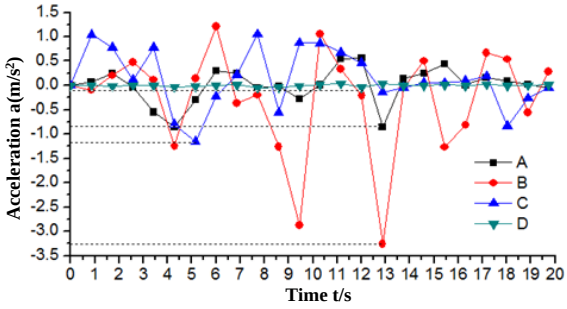

Figure 4. Acceleration Diagram of each Monitoring Point under Seismic Condition

It can be known from Figure 4 that, acceleration of each point is positive and negative fluctuation. Where acceleration of point D is the minimum, almost to be zero; the acceleration of point A is the second, and fluctuates within ±0.75m/s2;Point B and C are relatively larger, and fluctuate within±1.23m/s2. The acceleration of point B is the maximum, and fluctuates within±3.27m/s2. Analysis shows that the location of point B is the contact interface of silty clay and gravelly soil, and this interface is not stable, is extremely prone to landslides under the effect of seismic load.

3.3.2. The Seismic Condition Comparative Analysis: It can be known from Figure 5, under three kinds of seismic conditions, shear and strain increment are concentrated distribution on the structure interface of silty clay and gravelly soil. Under the seismic condition of Wenchuan earthquake,

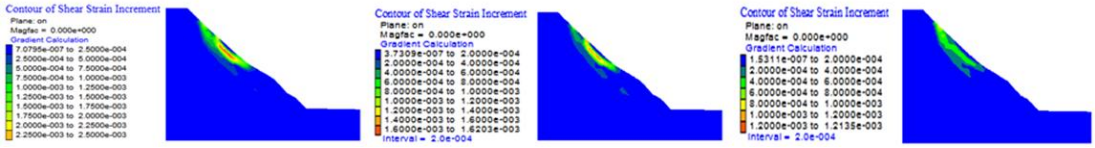

Figure 5. Shear and Strain Increment Nephogram of Various Seismic Conditions

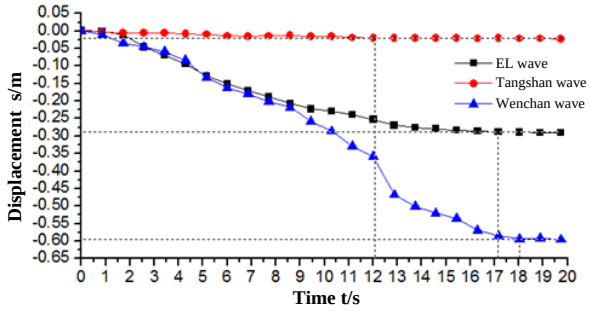

Figure 6. Displacement Diagram of Slope Waist Point B under Various Seismic Conditions

It can be known from Figure 6 that, under actions of different seismic waves, slope waist point B remained stable for a short time, the displacement increased, and enlarged gradually along with the increase of time, and the trend of displacement time-history curve of each point almost the same. Displacement of the condition of Wenchuan earthquake was the maximum, and achieved maximum 59 cm at 18 s; displacement of the condition of Elcentro earthquake was the second, and achieved maximum 29 cm at 17 s;

the displacement of the condition of Tangshan earthquake was the minimum, and achieved the maximum 2 cm at 12 s.

Figure 7 shows that, under different seismic waves, the acceleration of each waist monitoring point is different. Slope waist point B produces vibration changes after remaining stable for a short time. As the increase of time, the slope monitoring place has changes within a certain amplitude with their changing rule of seismic wave. Under the seismic condition of Wenchuan earthquake, the acceleration achieved the maximum 3.27m/s2 at 13s. Under the seismic condition of Elcentro earthquake, the acceleration achieved the maximum 2.1m/s2 at 7.7s. Under the seismic condition of Tangshan earthquake, the acceleration achieved the maximum 2.1m/s2at 6.1s.

It considered from the analysis that, the displacement of soil of point B (silty clay) had great difference under seismic dynamic loading effect, its characterization shown larger relative displacement, namely soil was destroyed at point B. Based on above analysis, the strain increment of contact interface of silty clay and gravelly soil was 2.5×10-3；under the seismic condition of elcentro earthquake, the maximum shear and strain increment of slope body shall be 1.62×10-3；under the seismic condition of Tangshan earthquake, the maximum shear and strain increment of slope body shall be 1.2×10-3.

Analysis shows that, under different seismic conditions, the maximum shear and strain increment are different, but are all concentrated in the waist, to characterize the seismic condition, slope waist loosely, stability declines, and sliding trend is obvious. Is not stable, it is extremely prone to landslides under seismic load effect due to instability.

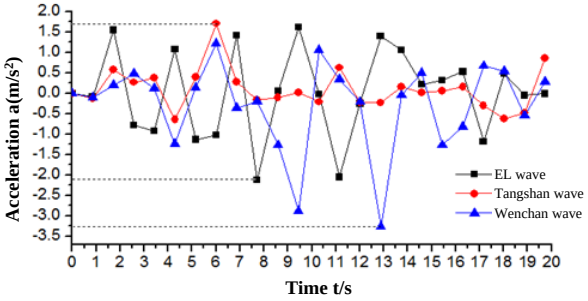

Figure 7. Acceleration Diagram of Slope Waist Point B under Various Seismic Conditions

4. Conclusion

This paper adopted FLAC3Dmodel combined with grey vector machine to carry out modeling analysis on high slope of Shenhua BaoRi XiLe open-pit coal mine in detail, and simulated three different working conditions of natural, rainfall, earthquake, at the same time considering the sudden and randomness of earthquake, it simulated the influence of three kinds of earthquake working conditions on slope, and the overall and profile displacement fringe, shear and strain increment nephogram, displacement diagram of each monitoring point, the earthquake acceleration time-histories of slope under various conditions, and evaluated and analyzed the stability of slope. Through analysis on the stability of slope, the strength reduction safety factors table of the natural condition and different rainfall conditions was obtained, which provided the basis for the quantitative analysis of the relationship between rainfall and landslide. By assuming different earthquake conditions, and simulating the stress and strain status of slope in seismic condition, the dynamic characteristics of the monitoring point was obtained, and thus the relative changes of the slope at each position was obtained quantitatively. This paper simulated the slope body of XiLe open-pit coal mine, provided theoretical basis for slope stability analysis under complicated conditions.

References

[1] D. Jiang, X. Ying, Y. Han, "Collaborative multi-hop routing in cognitive wireless networks[J]", Wireless Personal Communications, **(2015)**, pp. 1-23.
[2] J. Hu and Z. Gao, "Modules identification in gene positive networks of hepatocellular carcinoma using Pearson agglomerative method and Pearson cohesion coupling modularity[J]", Journal of Applied Mathematics, 2012 **(2012)**.
[3] D. Jiang, Z. Xu, Z. Chen, "Joint time-frequency sparse estimation of large-scale network traffic[J], Computer Networks, 2011, 55(15): 3533-3547.Jinyu Hu, Zhiwei Gao and Weisen Pan. Multiangle Social Network Recommendation Algorithms and Similarity Network Evaluation[J]. Journal of Applied Mathematics, 2013 **(2013)**.
[4] M. Zhou, G. Bao, Y. Geng, B. Alkandari, X. Li, "Polyp detection and radius measurement in small intestine using video capsule endoscopy", 2014 7th International Conference on Biomedical Engineering and Informatics (BMEI), Oct. **(2014)**.
[5] G. Yan, Y. Lv, Q. Wang, Y. Geng, "Routing algorithm based on delay rate in wireless cognitive radio network", Journal of Networks, vol. 9, no. 4, pp. 948-955, Jan. **(2014)**.
[6] Y. Lin, J. Yang, Z. Lv, "A Self-Assessment Stereo Capture Model Applicable to the Internet of Things[J]", Sensors, **(2015)**, vol. 15, no. 8, pp. 20925-20944.
[7] K. Wang, X. Zhou, T. Li, "Optimizing load balancing and data-locality with data-aware scheduling[C]", Big Data (Big Data), 2014 IEEE International Conference on. IEEE, **(2014)**, pp. 119-128.
[8] L. Zhang, B. He, J. Sun. "Double Image Multi-Encryption Algorithm Based on Fractional Chaotic Time Series[J]", Journal of Computational and Theoretical Nanoscience, **(2015)**, 12, pp. 1-7.
[9] T. Su, Z. Lv, S. Gao, "3d seabed: 3d modeling and visualization platform for the seabed[C]", Multimedia and Expo Workshops (ICMEW), 2014 IEEE International Conference on. IEEE, **(2014)**: pp. 1-6.
[10] Y. Geng, J. Chen, R. Fu, G. Bao, K. Pahlavan, "Enlighten wearable physiological monitoring systems: On-body rf characteristics based human motion classification using a support vector machine", IEEE transactions on mobile computing, vol. 1, no. 1, pp. 1-15, Apr. **(2015)**.
[11] Z. Lv, A Halawani, S. Feng, "Multimodal hand and foot gesture interaction for handheld devices[J]", ACM Transactions on Multimedia Computing, Communications, and Applications (TOMM), **(2014)**, 11(1s): 10.
[12] G. Liu, Y. Geng, K. Pahlavan, "Effects of calibration RFID tags on performance of inertial navigation in indoor environment", 2015 International Conference on Computing, Networking and Communications (ICNC), Feb. **(2015)**.
[13] J. He, Y. Geng, Y. Wan, S. Li, K. Pahlavan, "A cyber physical test-bed for virtualization of RF access environment for body sensor network", IEEE Sensor Journal, vol. 13, no. 10, pp. 3826-3836, Oct. **(2013)**.
[14] W. Huang, Y. Geng, "Identification Method of Attack Path Based on Immune Intrusion Detection", Journal of Networks, vol. 9, no. 4, pp. 964-971, Jan. **(2014)**.
[15] X. Li, Z. Lv, J. Hu. XEarth: A 3D GIS Platform for managing massive city information[C]. Computational Intelligence and Virtual Environments for Measurement Systems and Applications (CIVEMSA), 2015 IEEE International Conference on. IEEE, **(2015)**, pp. 1-6.

Authors

Liu Bo, Professor of School of Mechanics and Civil Engineering, China University of Mining & Technology (Beijing) China. He mainly engaged in the research and teaching work in urban underground engineering, geotechnical engineering and numerical analysis, foundation engineering, building materials and engineering management. He published more than 40 papers as the first author in the domestic and international journals and international academic conferences.